Anal. Chem. **2004,** *76,* 5063−5068

On-Chip High-Pressure Picoliter Injector for Pressure-Driven Flow through Porous Media

David S. Reichmuth, Timothy J. Shepodd, and Brian J. Kirby*

Sandia National Laboratories, Livermore, California, P.O. Box 969 MS 9951, Livermore, California 94551

A high-pressure (>3 MPa) on-chip injector has been developed for microchip applications including HPLC. The mechanical injector is implemented using in situ photopolymerization of fluorinated acrylates inside wet-etched silica microchips. The injector allows reproducible injections as small as 180 pL with <250 ms duration. The injector operated robustly over 60 days and over 1000 injections. The injector is unique among polymer-based valves as it functions in aqueous, acetonitrile, and mixed buffers at high pressures without detectable leakage.

Control of fluids at the microscale is fundamental for enabling microfluidic systems of increasing complexity. Recent research has demonstrated the ability to route pressure-driven flows at low pressure, and these methods of fluid control have been used for microfluidic injections,[1,2] peristaltic pumping, isolation of reaction zones,[3] and cell sorting.[4] In this work, we report on-chip pressure injections of subnanoliter volumes for high-pressure (>3 MPa) analytical applications. Our injector is the first system suitable for precise metering of high-pressure flows of both aqueous and organic solvents.

Minimizing injection volumes decreases the length of time required for separation, decreases the size of the separation device, and increases separation resolution. Therefore, improvements in the injection size can lead to significant overall improvements in microanalytical devices. A number of on-chip injection methods exist for systems that incorporate electroosmotic flow,[5−7] and these are useful in a number of applications. However, many analytical systems are incompatible with EOF-based injections, the foremost being HPLC-based analysis methods.

HPLC is a well-characterized and robust method for chemical and biomolecule identification and quantification and is the standard for many biochemistry and proteomic experiments. A wide variety of separation media exists, allowing compounds to be distinguished via a number of properties. However, the production of a microfluidic HPLC system requires pressure injections of volumes significantly less than the void volume of the separation column. Also, the dead volume between the injection and the separation column must be small to avoid significant sample dispersion. Subnanoliter on-chip injections are the critical enabling technology for HPLC in a microfluidic chip format.

The operational requirements for injector systems for HPLC are quite stringent. The materials must be compatible with a range of aqueous and organic liquids, including ionic buffers, acetonitrile, methanol, and organic acids. The injection must be rapid and reproducible, and the injection cycle time must be shorter than the duration of the HPLC analysis itself. In addition, the materials must be inert with respect to the analyte and buffer.

The microfluidic injector presented here is uniquely capable of handling subnanoliter volumes of aqueous and organic solvents at pressures typically used for flow through porous chromatography media. Currently, attempts to adapt pressure-based analyses (such as HPLC) to a microchip format require the use of conventional, off-chip sample definition.[8] The large volume and dead time introduced by an off-chip injection hinder the ability of a microfluidic-based separation to deliver rapid and sensitive analyses. The few examples of pressure-driven injections at the microfluidic scale are unsuitable for facile high-pressure injection.[9−11] Use of elastomer-based microfluidic valves has been demonstrated for low-pressure chromatographic separations in aqueous systems;[12] however, elastomers deform in response to pressure, preventing high-pressure world-to-chip connections and creating fluidic capacitance that degrades separation performance. In addition, most elastomers are incompatible with the organic solvents and acids commonly used in HPLC separations; a substantial fraction of their weight can be removed by solvents,[13] making mass spectrometric detection difficult. Several hydrogel

* Corresponding author. Current address: Sibley School of Mechanical and Aerospace Engineering, Cornell University. E-mail: bk88@cornell.edu.

(1) Blom, M. T.; Chmela, E.; Gardeniers, J. G. E.; Tijssen, R.; Elwenspoek, M.; van den Berg, A. *Sens. Actuators, B* **2002**, *82*, 111−116.
(2) Vahey, P. G.; Park, S. H.; Marquardt, B. J.; Xia, Y.; Burgess, L. W.; Synovec, R. E. *Talanta* **2000,** *51*, 1205−1212.
(3) Unger, M. A.; Chou, H. P.; Thorsen, T.; Scherer, A.; Quake, S. R. *Science* **2000**, *288*, 113−116.
(4) Fu, A. Y.; Chou, H.-P.; Spence, C.; Arnold, F. H.; Quake, S. R. *Anal. Chem.* **2002**, *74*, 2451−2457.
(5) Lazar, I. M.; Karger, B. L. *Anal. Chem.* **2002**, *74*, 6259−6268.
(6) Cannon, D. M., Jr.; Kuo, T.-C.; Bohn, P. W.; Sweedler, J. V. *Anal. Chem.* **2003**, *75*, 2224−2230.
(7) Harrison, D.; Manz, A.; Fan, Z.; Ludi, H.; Windmer, H. *Anal. Chem.* **1992**, *64*, 1926−1932.
(8) Killeen, K.; Yin, H.; Sobek, D.; Brennen, R.; Goor, T. v. d. In *Micro Total Analysis Systems 2003*, Proceedings of the 7th International Conference on Micro Total Analysis Systems, Squaw Valley, California, Oct 5−9, 2003; Northrup, M. A., Jensen, K. F., Harrison, D. J., Eds.; Transducers Research Foundation: Cleveland Heights, OH; pp 481−484.
(9) Gorbounov, V.; Kuban, P.; Dasgupta, P.; Temkin, H. *Anal. Chem.* **2003**, *75*, 3919−3923.
(10) Grover, W. H.; Skelley, A. M.; Liu, C. N.; Lagally, E. T.; Mathies, R. A. *Sens. Actuators, B* **2003**, *89*, 315−323.
(11) Backofen, U.; Matysik, F.; Lunte, C. *Anal. Chem.* **2002**, *74*, 4054−4059.
(12) Vahey, P. G.; Smith, S. A.; Costin, C. D.; Xia, Y.; Brodsky, A.; Burgess, L. W.; Synovec, R. E. *Anal. Chem.* **2002**, *74*, 177−184.
(13) Lee, J. N.; Park, C.; Whitesides, G. M. *Anal. Chem.* **2003**, *75*, 6544−6554.

10.1021/ac0493572 CCC: $27.50
Published on Web 07/28/2004

valve architectures have been successfully demonstrated, first for low-pressure applications[14] and more recently for holding off high pressures in capillaries.[15] Even the high-pressure work, though, has not demonstrated the ability to inject small samples at high pressure—the thermoresponsive hydrogel elements presented to date[15] may be difficult to adapt to high-pressure microchip HLPC injections since the pressure holdoff required extremely large (5000 μm) elements, leading to significant dead volumes. Also, the swelling phenomena required for thermoresponsive valve actuation is dependent on the solvent hydrophobicity, so operation in HPLC solvents may be affected. Further, while bulk flow can be affected by hydrogel barriers, diffusive transport is still present and can lead to contamination between lines.

Earlier work using values constructed from mobile photopolymerized polymer elements overcame the high-pressure limitations of other work and demonstrated the ability of mobile monolithic polymer structures to route organic fluids,[16,17] but an architecture for subnanoliter microchip injections suitable for HPLC has not been previously demonstrated. The values in previous work[16,17] operated only with mobile phases with >90% organic solvent, since the polymers used contracted if the aqueous component was increased, and even minor contraction can lead to increases in leak rate by factors of 10^2−10^6. Because most separations are performed in predominantly aqueous buffers, these fluidic control schemes were unsuitable for injection in the presence of standard HPLC solvents. Further, previous microchip injectors[16] had volumes not significantly lower than the smallest capillary systems (~10 nL) and quoted leak rates (160 pL/s) approximately 3 orders of magnitude greater than that required for repeated injections of uniform subnanoliter volumes.

Here we demonstrate the fabrication of a microfluidic injector suitable for application to microchip HPLC separations via in situ polymerization of a ~150-μm monolithic phase-separated fluorinated acrylate inside the channels of a fused-silica microchip. This injector allows small-volume injections at high pressure by creating a mobile polymer element that moves in response to pressure differentials and seats when compressed against channel restrictions. The valve element in this injector is topologically similar to microfluidic valving presented previously,[16,17] but it is reduced in size and incorporates recent materials developments.[18] Compared to previous work,[16] the present system performs injections that are approximately 2 orders of magnitude smaller than previous work (from 10 nL to 180 pL) and demonstrates leak rates reduced by 3 orders of magnitude at similar pressure differentials (from 160 pL/s to below 0.2 pL/s). This reduction in leak rate enables repeatable picoliter-sized high-pressure injections that are unaffected by any contamination between lines. In addition to HPLC applications, this valve could also be used for other on-chip applications that would require leak-free fluid routing, such as reaction isolation and postseparation switching.

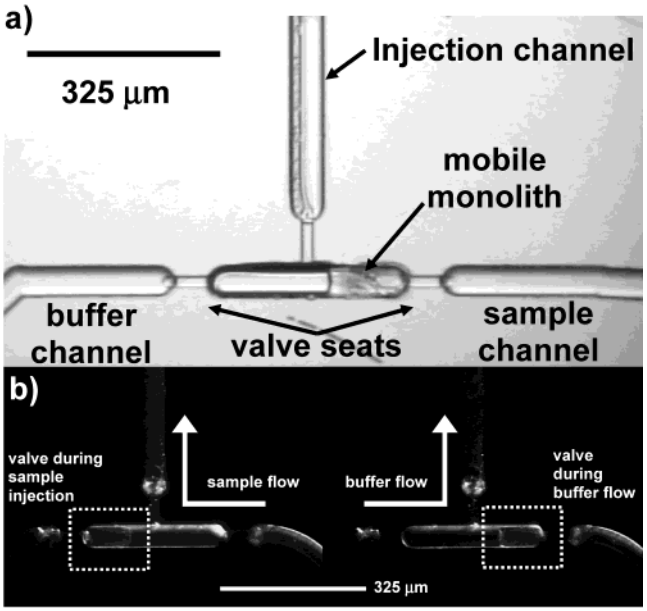

Figure 1. (a) Micrograph of the injection valve. In the position shown, fluid from the buffer input at left travels down the injection channel at top. Sample fluid at right is isolated from the rest of the system. (b) Movement of the polymer element (mobile monolith) allows control of the fluidic pathways.

MATERIALS AND METHODS

Chemicals. 2,2,3,3-tetrafluoro-1,4-butanediol diacrylate (TFBDDA) was purchased from Monomer−Polymer & Dajac Laboratories Inc. (Feasterville, PA). Glacial acetic acid, 3-(trimethoxysilyl)-propyl acrylate, 1,4-dioxane, 2,2′-azobisisobutyronitrile (AIBN), acetonitrile (ACN), 2,2,2-trifluoroethyl acrylate (TFEA), and 2,2,3,3,4,4,4-heptafluorobutyl acrylate (7FBA) were purchased from Sigma-Aldrich (St. Louis, MO). RhodamineCl 560 was purchased from Exciton (Dayton, OH). Fluorinert FC-84 was obtained from 3M (St. Paul, MN). Tridecafluoro-1,1,2,2,-tetrahydrooctyl-triethoxysilane (TDFTES) was purchased from Gelest, Inc. (Tullytown, PA), and heptafluorobutyric acid (HFBA) was obtained from Pierce Biotechnology (Rockford, IL).

Wafer Fabrication. Silica microchips were fabricated from Corning 7980 fused-silica wafers of 100-mm diameter and 0.75-mm thickness (Sensor Prep Services, Inc., Elburn, IL) using standard photolithography, wet etch, and bonding techniques.[18] Multiple etch processes are used to create the 3-D geometry desired for valve operation. The bottom wafer is etched in two separate steps. The first etch is of 20-μm depth nominal with a photomask that exposes the microchannels and valve regions. The etch process is repeated a second time with a second photomask—a 5-μm depth nominal etch connects the valve regions to the microchannels, allowing a fluidic connection while simultaneously providing for the constriction required to create a valve seat (Figure 1). The cover wafer (which has the access holes drilled before etch steps) is etched only in the valve regions. Following etch steps, the bottom and cover wafers are aligned to a precision of 3−5 μm using a mask aligner and are thermally bonded for 5 h at 1150 °C in a N_2-purged programmable furnace (Thermolyne, Dubuque, IA).

Fabrication of Integrated Microvalve Injector and Fluidic Resistance. The integrated microvalve injector and a monolithic porous polymer structure were both fabricated in situ using

(14) Beebe, D.; Moore, J.; Bauer, J.; Yu, Q.; Liu, R.; Devadoss, C.; Jo, B. *Nature* **2000**, *404*, 588.
(15) Luo, Q.; Mutlu, S.; Gianchandani, Y. B.; Svec, F.; Frechet, J. M. J. *Electrophoresis* **2003**, *24*, 3694−3702.
(16) Hasselbrink, E. F., Jr.; Shepodd, T. J.; Rehm, J. E. *Anal. Chem.* **2002**, *74*, 4913−4918.
(17) Kirby, B.; Shepodd, T.; Hasselbrink, E. *J. Chromatogr., A* **2002**, *979*, 147−154.
(18) Kirby, B. J.; Reichmuth, D. S.; Renzi, R. F.; Shepodd, T. J.; Wiedenman, B. W. Lab Chip, submitted for publication, 2004.

photoinitiated free radical polymerization. The microvalve injector consisted of a monolithic polymer element fabricated within a three-dimensional microstructure formed from wet-etched microchannels in a fused-silica microchip. A photopolymerized monolithic porous polymer structure (similar to those reported elsewhere, e.g., refs 19 and 20) was fabricated to provide a high-fluidic-resistance pathway to evaluate the performance of the microvalve injector.

Construction of the integrated system involved two surface modifications and two polymerization steps, detailed in the paragraphs to follow. The internal surfaces of the chip were first functionalized with a fluorinated alkyl coating so as to generate a low-energy surface that leads to low friction coefficients when in contact with fluorinated acrylate materials.[18] The microchannel surfaces were coated via incubation for 45 min at 70 °C with a solution of 75% 1,4-dioxane, 12.5% glacial acetic acid, 10% TDFTES, and 2.5% deionized water, and then flushed with 1,4-dioxane followed by acetonitrile.

Following the fluorination surface treatment, the high-pressure microvalve injector was created by laser-photopatterning a free-standing polymer element within a microchannel as described previously.[18] A mixture of solvent, monomers, and photoinitiator was placed in the chip using vacuum. Four hundred microliters of monomer solution consisted of 124 μL of TFBDDA, 124 μL of 7FBA, 76 μL of TFEA, 76 μL of FC-84, and 4 mg of AIBN. The mixture was photopolymerized by projecting the output of a 12 kHz, 4 mW, 355-nm laser (Nanolase, JDS Uniphase) onto the microchip. The illuminated area was shaped with a series of lenses and a mechanical slit to an approximately 150 μm $\times$ 600 μm rectangular region, and the polymerization occurred after 20−40 s of exposure. Polymerization was monitored via visual inspection with a CCD camera fitted with a microscope objective. Laser exposure was terminated when the phase interface between the solid polymer monolith and the liquid monomer solution became visible (Figure 1). After polymerization, the chip was flushed with acetonitrile.

Following valve fabrication, a second surface coating was performed to enable covalent attachment of a long (1.7 cm) monolithic porous polymer within the output microchannel. This porous polymer served as a flow restrictor and emulates the flow restriction attendant with porous or packed particle bead systems used for chromatography or surface-catalyzed reaction. The microchannels were filled with a solution consisting of 40% glacial acetic acid, 40% deionized water, and 20% 3-(trimethoxysilyl)propyl acrylate and incubated at room temperature for 30 min. The chip was then flushed with acetonitrile. Finally, a fixed, porous monolith was polymerized downstream of the injection valve, using contact lithography.[21,22] This fixed monolith provides significant fluidic resistance, with a pressure drop of 560 psi (3.9 MPa) at a flow rate of 1 nL/s.

High-Pressure Microfluidic Connections. Once the high-pressure microvalve injector and downstream fluidic resistance were integrated at chip-level, connections to external pressure sources were made using custom-designed high-pressure fittings and capillary connections.[18] Female ULTEM fittings with incorporated Buna-N O-rings were epoxied to the chip; these fittings are leak-tight to approximately 6.40 MPa (1000 psi). The fittings were reversibly connected to 350-μm OD capillary tubing via a hand-tightened, compression-sealed PEEK ferrule. Stainless steel hypodermic tubing (28 gauge, Microgroup, MA) was used for most connections due to its structural integrity. Glass capillaries (Polymicro, Phoenix, AZ) were used when small ID connections were required.

Valve Operation and External Pressure Sources. The valve function is achieved via the movement of the mobile polymer monolith between constrictions in the fluid channels. Application of a pressure differential actuates the valve element (Figure 1). The physical restriction of flow caused by blockage of the channel enables reversible fluidic routing. In addition, casting the valves inside the channel gives the polymer element the exact dimensions of the channel and therefore allows for leak-free switching. The actuation of the valves is implemented simply by control of the fluid pressure difference in the channels, which can be easily implemented on-chip or externally.

External pressure sources were used to drive flow through the fixed monolithic porous structure and control and actuate the high-pressure microvalve injector (Figure 2). One input channel (termed the "buffer channel" in anticipation of miniaturized HPLC injector applications) was connected to a capillary and pressurized using a spring-powered syringe pump. The other input channel (termed the "sample channel") was pressurized via a spring-powered syringe pump and connected to the chip through an electronically controlled switching valve (C1-2006,VICI, Houston, TX). The switch allowed rapid external pressurization/depressurization of the sample channel by input selection between the pressurized syringe pump and an open port. The valve was controlled using a gate/delay generator (DG-535, Stanford Research Systems, Sunnyvale, CA) allowing selection of the pulse width and frequency.

Visualization and Image Processing. Device performance was evaluated using epifluorescence imaging of dye solution injected into a running system of dye-free solution. An argon ion laser (Ominchrome) operating at 488 nm illuminated the field-of-view of a color CCD (Sony XC999) fitted with a 5× microscope objective (Mututoyo). A 488-nm HR, 510-nm LP dichroic mirror was used to introduce the laser light and filters (CG 530, Schott; 488-nm holographic notch, Kaiser) were used to isolate the sample fluorescence. Solutions of 2.5 μg/mL rhodamine in 30% ACN/70% deionized water/0.1% HFBA were used to visualize the injections. The buffer channel was filled with 30% ACN and 0.1% HFBA in 5 mM phosphate buffer at pH 6.8. Movies were recorded in 640 $\times$ 480 $\times$ 16 bit resolution at 15 Hz using a PC running Virtualdub 1.5.3 (www.virtualdub.org), and the data was processed using Matlab 6.1 (The Mathworks Inc., Natick, MA).

The volume of fluid injected was calculated by comparing the integrated intensity of the injected fluid to a known volume. An example of a single frame from a movie is shown in Figure 3. The image intensity over the area containing the valve output channel and the buffer channel (region 1) was integrated to determine the quantity of sample injected. The integrated image intensity of a known fluid volume in the sample channel (region

(19) Yu, C.; Davey, M.; Svec, F.; Frechet, J. *Anal. Chem.* **2001**, *73*, 5088−5096.
(20) Ngola, S. M.; Fintschenko, Y.; Choi, W.-Y.; Shepodd, T. J. *Anal. Chem.* **2001**, *73*, 849−856.
(21) Yu, C.; Svec, F.; Frechet, J. M. J. *Electrophoresis* **2000**, *21*, 120−127.
(22) Shediac, R.; Ngola, S. M.; Throckmorton, D. J.; Anex, D. S.; Shepodd, T. J.; Singh, A. K. *J. Chromatogr., A* **2001**, *925*, 251−263.

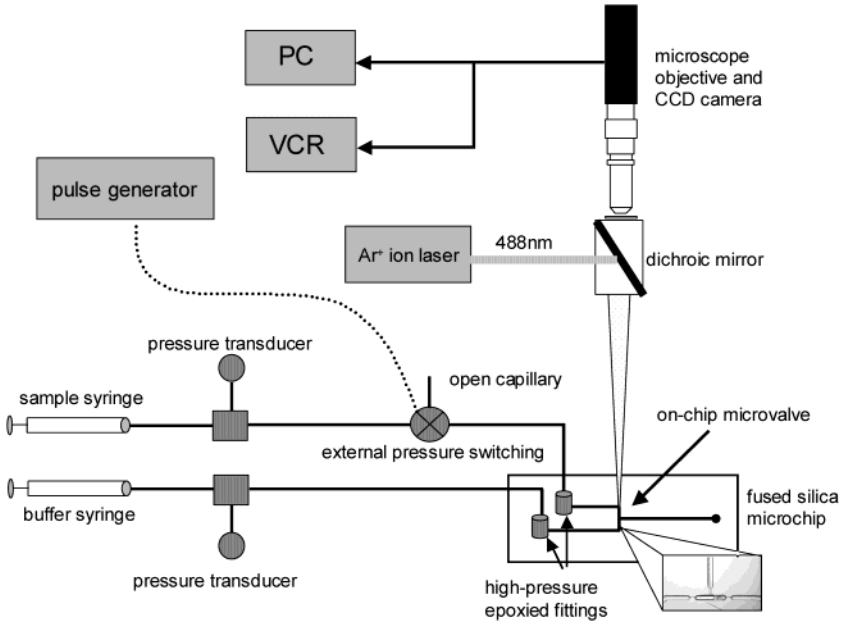

Figure 2. Schematic of the injection quantification apparatus.

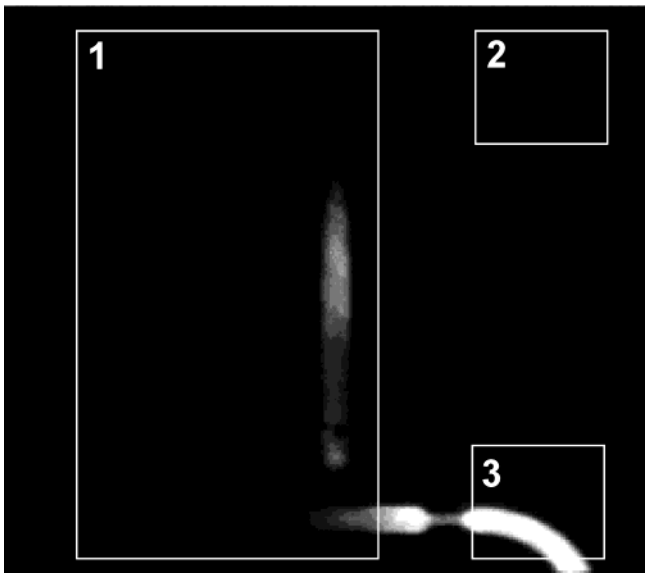

Figure 3. Micrograph of the injection valve with the integration areas highlighted. The integrated signal from region 1 is due to the flow of dye solution into the injection channel and is used to calculate the injected volume. Signal measured in region 2 is used to determine background fluorescence. Region 3 comprises a known volume of sample, allowing calibration of fluorescence intensity to volume of solution injected.

3) was also calculated. This value was used to establish a relationship between the integrated image intensity and the volume of sample present. Since the sample channel concentration was constant and known, variations in the intensity of the sample channel were used to infer temporal fluctuations in the laser intensity and thus remove laser power fluctuations from the final volume calculation. A third region of the chip (region 2), in a region without fluidic channels, was used to establish the background intensity. The average background signal was subtracted from both the sample and injection regions. This series of calculations were carried out for each frame in the movie and was used to determine the volume of sample injected at each time step.

Fluorescence downstream of the valve was also measured through epifluorescence microscopy. Three rows of each frame were integrated and the background signal removed. The rows chosen were downstream of the valve, and the results replicate the behavior of a fixed slit fluorescence detector.

RESULTS AND DISCUSSION

Valve Fabrication and Operation. An integrated system was fabricated that included external pressure sources, on-chip fluid injector valve, and downstream flow resistance, and this system was used to demonstrate and evaluate the performance of the high-pressure hydraulic injector valve under conditions that mimic miniaturized HPLC conditions. The injection valve (Figures 1 and 2) functions by allowing selection of pressure-driven flow from one of two input channels. This selection occurs via movement of the polymer element so that a seal is created between the polymer and the shallow-etched valve seats. Because the device is created by in situ polymerization and the polymer exhibits little change in size after formation, the monolith is precisely shaped to the channel dimensions. The monolith moves in response to a pressure differential of >10 psi (69 kPa) between the input channels, and an effective seal forms when the pressure difference is >100 psi (689 kPa). Sealing occurs when the larger, cylindrical polymer element is held against the smaller, hemi-cylindrical channel. The pressure differential is sufficient to stop fluid from flowing between the polymer element and the channel wall. Typical operation of the injection valve uses a constant pressure on the buffer channel, with step changes in the sample channel pressure. The injection takes place when a pressure >100 psi greater than the buffer channel is applied to the sample for a brief period. Ideally, the sample pressure is varied from atmospheric pressure to the injection pressure in a square pulse.

This valve architecture shows an extraordinarily low leak rate, which uniquely enables high-pressure injection through porous media. Successful implementation of the injection valve requires

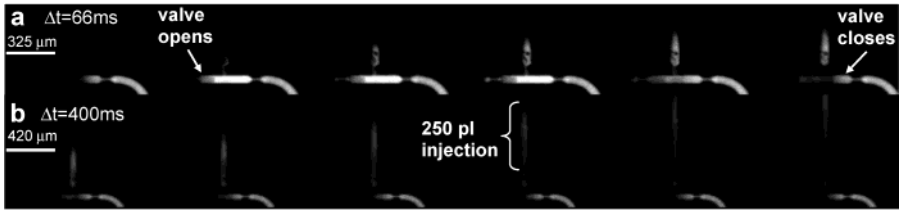

Figure 4. Time series of a 250 pL injection. Series a shows the opening and closing of the injection valve. While the motion of the polymer element cannot be seen directly, the presence of fluorescence in the injection region is indicative of valve actuation. Series b displays the movement of the sample plug into the injection channel.

that the volume leaking from the buffer channel into the sample channel be insignificant for the duration of the injection and analysis cycle. At a high leak rate, the sample fluid would be displaced from the sample channel, resulting in contamination of the injected samples. Our measurements showed no discernible leak of buffer into the sample channel with any sample fluid; a range of 0% to 40% acetonitrile in water was tested in detail in anticipation of reversed-phase chromatography applications.

The injector valve has performed reproducibly over thousands of injections, and delays between injections have been varied between 1 s and 1 week without significant change in performance. Visible signs of leakage could not be observed when the input channel pressure differential was greater than 100 psi (689 kPa). No change was observed in the sample channel after pressure was applied on the buffer line for 168 h, indicating that the sample mass flux caused by any leak rate (if present) was insignificant compared to the diffusive mass flux of the dye in the buffer line. The maximum leak rate that would be completely masked by steady-state diffusion is estimated to be 0.2 pL/s, indicating that the leak rate of this valve, if any, is below this value. The initial injection after 168 h of inactivity had an injection volume within 6% of the size of the injections recorded earlier. The error is comparable to the 5% average variation seen between repeated injections performed at 0.1 Hz. The leak rate of this polymer monolith is 700-fold smaller than that quoted for earlier valves,[16] enabling repeatable subnanoliter injections. The absence of measurable leaks at elevated pressures is unique for a solvent-compatible microchip valve architecture and makes this architecture suitable for applications such as on-chip HPLC.

Valve Performance. Two series of micrographs (Figure 4) taken from a video (video S1 in the Supporting Information) recorded during injection illustrate the operation of the microvalve injector and highlight the quality of the valve performance. The initial micrograph shows the dye sample in the right channel at atmospheric pressure while nonfluorescent buffer solution is flowing from the left channel at 300 psi. The absence of dye dilution or displacement evinces the effective isolation of the two liquid lines. The following five frames depict the injection of the fluorescent sample as the right-side (sample) channel is pressurized to 450 psi. In the second series, the valve again isolates the buffer from the sample, and the Poiseuille flow of injected dye can be seen moving downstream from the valve region. The area immediately downstream of the valve was intentionally left open to facilitate these measurements. In future devices, this open area can be eliminated to reduce dispersion between the injector and separation medium.

The time history of the injected sample volume can be straightforwardly measured by fluorescence microscopy (Figure 5). At the start of the 250 ms, 220 pL injection cycle, the buffer channel is at 300 psi and the monolith valve element isolates the sample channel from the rest of the system. No measurable fluorescence can be observed in the injection channel or valve region. At 1.2 s, the sample channel is pressurized to 450 psi and the mobile polymer element is displaced to the left (Figure 1b) and seats against the buffer channel. The volume of sample in the valve and injection channel increases during the 200 ms period that the valve is open. The pressure applied to the sample channel is then reduced to atmospheric pressure, and the polymer element returns into position to seal the sample channel. During the closing of the injection valve, much of the sample material in the valve region is pushed back into the sample channel, resulting in a decrease in the calculated sample volume at the time of valve closure. The net effective injection volume is indicated by the volume result immediately following valve closure. The volume inside the field-of-view decreases starting at 2 s as the flow moves the sample out of the field-of-view.

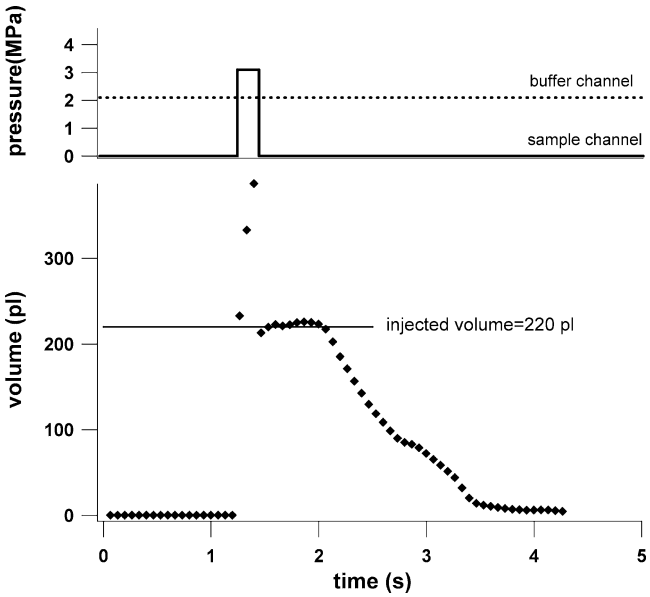

Figure 5. Volume of sample fluid present in the valve region and injection channel during an injection cycle, indicated with diamond markers. The volume of sample fluid is calculated from the fluorescence, as shown in Figure 3. The injection volume is 220 pL. The buffer channel (dashed line) is held at constant pressure, 2.1 MPa (300 psi). The sample channel (solid line) is pressurized to 3.1 MPa (450 psi) at 1.20 s and depressurized at 1.46 s.

The performance of the valve can also be demonstrated by measuring the flow of fluorescent dye through a point downstream of the valve. Figure 6 shows the resulting peaks in fluorescence generated by a series of injections. The valve produces evenly

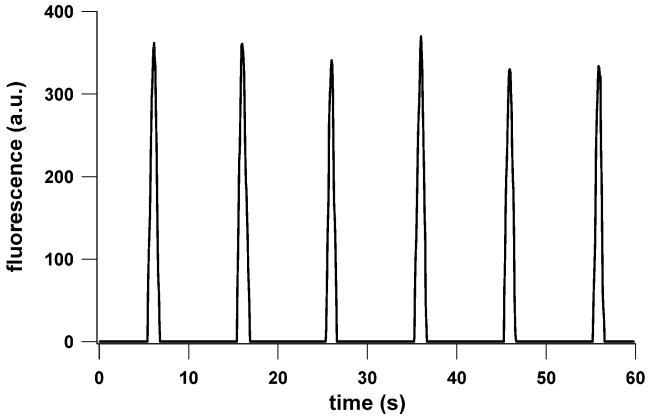

Figure 6. Fluorescence intensity measured downstream from the valve. Injections are performed at 0.1 Hz, with a 500 ms duration. The buffer channel is held at constant pressure, 2.1 MPa (300 psi); the sample channel is pressurized to 3.1 MPa (450 psi) during injection.

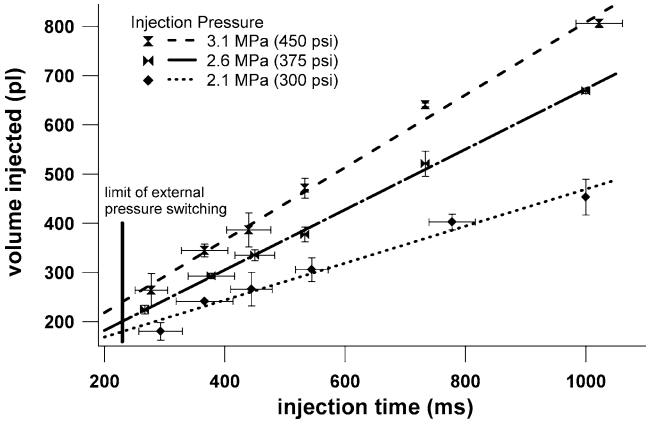

Figure 7. Injected volume as a function of injection time and pressure. The buffer channel pressure is held constant at 1.0 MPa (150 psi) below the injection pressure. Error bars indicate the standard deviation of the injection volume and duration.

spaced peaks and isolates the sample channel effectively. The ability to create repeatable injection pulses is directly applicable to numerous separation methods.

The ability of this microvalve injector to provide reproducible, metered injections at volumes as low as 180 pL was demonstrated by performing and evaluating a series of injections with varying injection time and pressure. All injections were made with a 150 psi pressure differential between the two input lines. Three injection pressures were tested, and at least three injections were measured at each combination of injection length and pressure. Figure 7 displays the average volume injected as a function of injection duration (250−1000 ms), using data collected from 124 injections. The injected volumes span a range from 180 to 806 pL. The volume of sample injected varied linearly with the length of injection time for each pressure tested. The uncertainty in the length of injection is in large part due to the finite (15 Hz) video capture rate. The system shows stable and reproducible injections over a period of months and thousands of injections. Injections of longer than 1 s are easily accomplished, but no attempt was made to quantify them using our current fluorescent imaging apparatus. The actuation time of the mobile polymer element was <10 ms, so the minimum injection duration was set by the performance limitations of the external pressure switching; with faster external pressure switching, injections of smaller volumes can be straightforwardly achieved.

CONCLUSIONS

The range, small size, and reproducibility of the high-pressure injections demonstrated here provide unique capabilities for microscale analytical systems. Because the valve system operates at high pressures and in a range of solvents, it is particularly well suited for HPLC applications. High-pressure fluidic injections have been performed with 0−40% ACN/water mixtures with minimum volumes of 180 pL at pressures near 3 MPa and leak rates below 0.2 pL/s. As compared to previous work with similar architectures,[16] these injections are roughly 2 orders of magnitude smaller in volume, and the observed leak rates are roughly 3 orders of magnitude lower. Further, new materials[18] allow these architectures related to previous work[16,17] to be applied to solvent systems useful for a broad range of HPLC separations.

Improvements to the current design can be made in speeding valve actuation and sample/buffer fluid changes. The temporal and minimum-volume performance of the valve is currently limited by the external pressure switching. Future work will include design of more precise macroscale components to facilitate accurate testing of the microdevices. Adding ports to the current three-port valve design will allow rapid buffer exchange in the sample or buffer lines without affecting the injection valve. The combination of this valve with an on-chip HPLC column will enable the fabrication of an integrated microchip HPLC system.

ACKNOWLEDGMENT

We thank R. F. Renzi for the design and fabrication of the high-pressure microfluidic packaging and fittings. This work was supported by the Laboratory Directed Research and Development program at Sandia National Laboratories. Sandia National Laboratories is a multiprogram laboratory operated by Sandia Corporation, a Lockheed Martin Company, for the United States Department of Energy under Contract DE-AC04-94AL85000.

SUPPORTING INFORMATION AVAILABLE

Video S1 (filename: 022004 reichmuth injector valve 250ms 450-300psi 0.167Hz .avi) showing a series of 260 pL dye injections as captured by epifluorescence microscopy. The video playback is in real time, and the injections were performed every 6 s. The injection duration was 250 ms, and dye was injected using a 450 psi pressure pulse from the channel on the right side of the valve. The buffer channel (left side of the valve) pressure was held constant at 300 psi. This material is available free of charge via the Internet at http://pubs.acs.org.

Received for review April 30, 2004. Accepted May 26, 2004.

AC0493572